

Orientation relationship between β -Si₃N₄ and Si in multicrystalline silicon ingots for PV applications

Espen Undheim¹, Per Erik Vullum², Randi Holmestad², Lars Arnberg¹, and Marisa Di Sabatino¹

1. Department of Materials Science and engineering, Norwegian University of Science and Technology (NTNU), 7491 Trondheim, Norway
2. Department of Physics, Norwegian University of Science and Technology (NTNU), 7491 Trondheim, Norway

Email: espen.undheim@ntnu.no

Abstract

The nucleation of Silicon in multicrystalline ingots cast in Si₃N₄ coated crucibles is thought to occur on β -Si₃N₄ particles. In this study the orientation relationship between Si and β -Si₃N₄ was investigated by transmission electron microscopy (TEM). The following orientation relation was found by analyzing diffraction patterns of the two phases.

$$[0001] \beta - Si_3N_4 \parallel [1\bar{1}1] Si$$

$$(\bar{4}5\bar{1}0) \beta - Si_3N_4 \parallel (011)Si$$

The particle, of which a TEM sample was prepared by a focused ion beam, was identified as a likely nucleation site based on the grain boundaries (GBs) extending from it. It was shown that these GBs were $\Sigma 3$ boundaries. The nucleation process has been discussed as a source for formation of twins in multicrystalline silicon.

1. Introduction

The industry standard today for the production of multicrystalline silicon (mc-Si) ingots for PV applications is to cast the material directly in silicon nitride (Si₃N₄) coated quartz crucibles by directional solidification. The role of the nitride coating is to prevent sticking between Si and the quartz crucible. The nitride coating commonly used by mc-Si producers is composed of mainly α -Si₃N₄ (> 95%) and small amounts of β -Si₃N₄ particles. The particles in this coating are small, with a size below 1 μ m [1].

Previous work by our group has shown that during solidification the α -phase undergoes a phase transformation to the β -phase. This causes the existing β -particles, as well as new particles, to grow. The β -phase particles grow to much larger sizes than the α -phase particles in the original coating, on the order of 10-20 μ m [2]. Our work shows that the larger β -particles are more favorable nucleation sites than the α -Si₃N₄ particles [1, 2].

The crystal structure of β - Si_3N_4 is hexagonal with a space group $P6_3/m$ and lattice parameters equal to $a = 7.61 \text{ \AA}$ and $c = 2,91 \text{ \AA}$ [3, 4]. The α -phase has a trigonal structure, with space group $P31c$ and lattice parameters $a = 7.75 \text{ \AA}$ and $c = 5.62 \text{ \AA}$ [5, 6].

β -particles grown from a silicon melt grow as hexagonal needles along the c -direction ($[0001]$ direction) [7, 8]. Epitaxial growth of β - Si_3N_4 on silicon has been studied both experimentally and theoretically [9-11]. Experimentally a Si/β - Si_3N_4 structure is created by nitridation of a silicon wafer, which gives a thin nitride layer [10, 11]. Both experimental and theoretical works focus on the $\text{Si} (111)$ and β - $\text{Si}_3\text{N}_4 (0001)$ interface. These interface planes give a low lattice mismatch (1%), where one unit cell of Si_3N_4 almost matches two unit cells of Si [9].

The β -particles found in mc-Si ingots do not show the (0001) facet, but show a more complex combination of facets [2]. The clearest facets that appear consistently for all particles are the side facets, and it is on these the nucleation is believed to occur. These facets are the $(10\bar{1}0)$, (1100) , and $(01\bar{1}0)$ planes and provide likely nucleation sites as the undercooling necessary for growth is dependent on the facet size, as suggested by athermal nucleation theory [12, 13].

Where Si nucleates on the β -phase particles there should be a preferred orientation relation (OR) between the two phases. In this work the OR between Si and β - Si_3N_4 particles has been studied in detail using transmission electron microscopy (TEM).

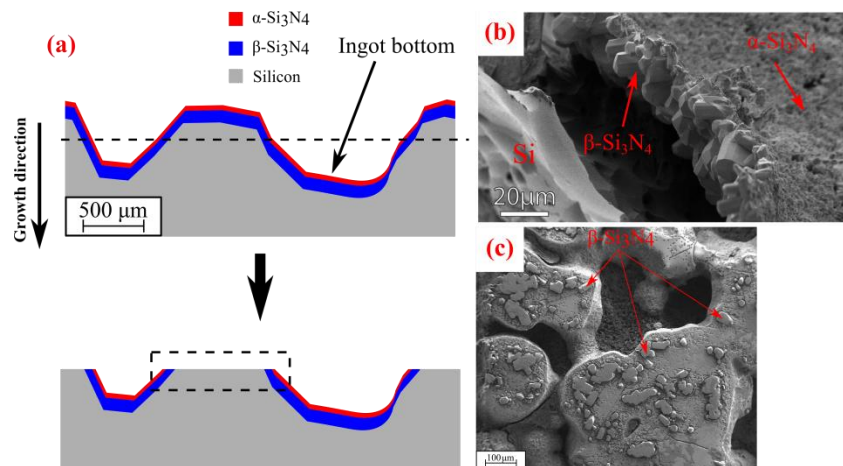


Figure 1 (a) Schematic of a bottom cut from a mc-Si ingot viewed from the side. The layers consist of α - and β - Si_3N_4 particles. The top image represents the sample before polishing, with the dotted line indicating the material removed during polishing. The bottom image is a schematic of the sample after polishing. The dotted area represents a so called Si “island”. (b) A real case example of the layers shown in (a). The micrograph is of an etched mc-Si sample from [2] (c) Example of the Si islands of a sample after polishing and etching. Also indicated are some of the β -particles.

2. Experimental

The TEM samples were prepared from bottom cuts of an industrial mc-Si ingot. Sample preparation of the bottom cuts was necessary in order to identify possible areas of interest for

TEM sample preparation. As reported by Ekstrøm et al. the bottom of mc-Si ingots is covered in a layer of α - Si_3N_4 particles [2]. This layer is followed by a layer of β - Si_3N_4 particles which are in contact with the silicon. This layer is a direct result of the phase transformation of the α - to β -phase. Figure 1 (b) shows these two layers and the underlying Si for an etched mc-Si sample from the study by Ekstrøm et al. [2]. In order to remove most of the α - Si_3N_4 layer, the samples were polished carefully, as to not remove too much of the underlying silicon. After the polishing, the sample consisted of silicon “islands” surrounded by remnants of coating particles. The polishing process removed less material than the roughness of the sample, creating Si islands, as shown in Figure 1. These islands are surrounded by β - Si_3N_4 particles on the outside border, and in some cases β -particles are found covering the islands, as seen in Figure 1 (c). The β -particles are identified based on size and shape.

After polishing the samples were etched in Sopori etchant for 15s to reveal the GBs. Areas for possible TEM sample lift-outs were identified by GBs extending from single β - Si_3N_4 particles. This is a sign that nucleation occurred on this particle and this is discussed in further detail in the next section. Cross-section TEM samples were prepared in a FEI Helios NanoLab DualBeam Focused Ion Beam (FIB) using the “lift-out” technique, shown in Figure 2. In this technique a carbon pad is first deposited on top of the area of interest to protect the sample area from damage during milling (Figure 2 (a)). The material around the sample is then milled away on three sides, as seen in Figure 2 (b), as well as beneath the sample, which is not visible in the figure. A needle is attached to the sample by platinum deposition and the final side milled away. The sample is then removed, shown in Figure 2 (c), and transferred to a copper grid (Figure 2 (d)). Here the sample is attached by deposited Pt and the sample is milled on both sides until it is electron transparent.

A JEOL 2100 microscope, operated at 200kV, was used to study the TEM samples. A Zeiss Ultra scanning electron microscope (SEM), operated at 2-5 kV, was used to identify areas of interest after polishing and etching.

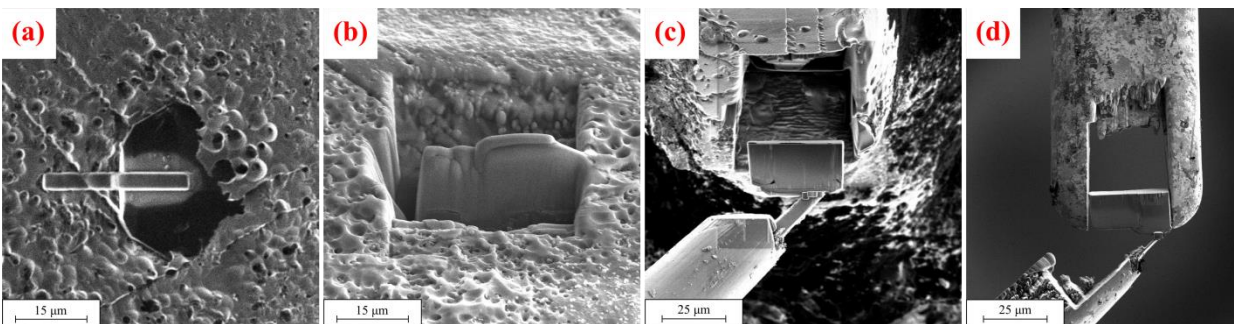


Figure 2: Micrographs roughly demonstrating the “lift-out” technique. (a) Deposition of a carbon pad to protect sample area. (b) Sample is milled out on the three sides visible in the micrograph, as well as beneath the sample. (c) A needle is attached to the sample by depositing Pt and the final side is milled. The sample is then lifted out. (d) The sample is moved to a copper grid and attached by Pt deposition.

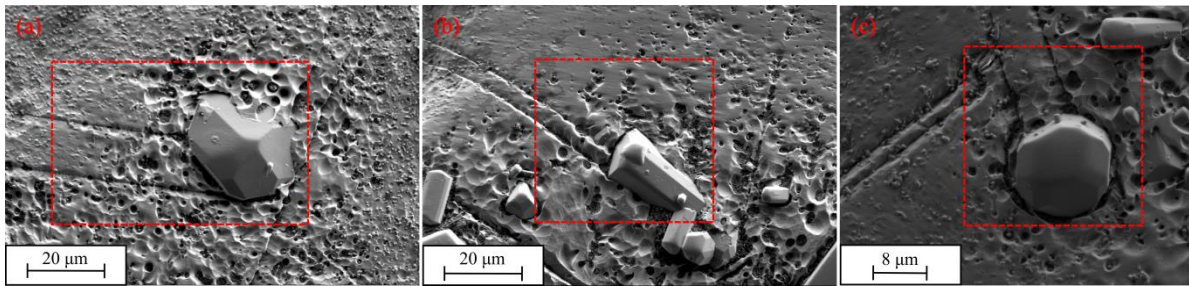


Figure 3 Areas of interest identified after sample preparation. Indicated inside the square are the suspected nucleating particle and grain boundaries extending from the particle.

3. Results and discussion

3.1. Areas of interest

Polishing and etching of the mc-Si bottom cuts revealed several interesting areas, with possibility for TEM sample preparation, shown in Figure 2. An assumption was made when looking for possible areas to study; that a particle could nucleate silicon on at least two facets of the same particle. For particles where Si nucleated twice, two GBs could be traced back to the particle, as can be seen in the examples shown in Figure 2 (a) – (c). For particles where Si only nucleated on one facet, it would be impossible to determine on which of the facets the nucleation started or even if Si nucleated on the particle at all. For nucleation on two or more facets, this could be decided with a much higher degree of certainty, e.g. in Figure 3 (a) and (c) GBs are seen to extend from the edges of one facet and thus it is highly likely that nucleation started on the facet bounded by the GBs.

In this study only one successful sample, i.e. a TEM sample that was good enough to be investigated and that also showed an OR, was made. This sample was made from the particle shown in figure 3 (a). The area where the TEM sample was made is shown in Figure 4 (a) with the areas of interest marked, the β -Si₃N₄ – Si boundary is shown by a red square and the Si-Si GB by a blue square. A bright field (BF) micrograph of the finished TEM sample is shown in Figure 4 (b), with the interface and the Si-Si GB marked. The coordinate system shows how the TEM sample is oriented in comparison to the ion beam micrograph in Figure 3 (a).

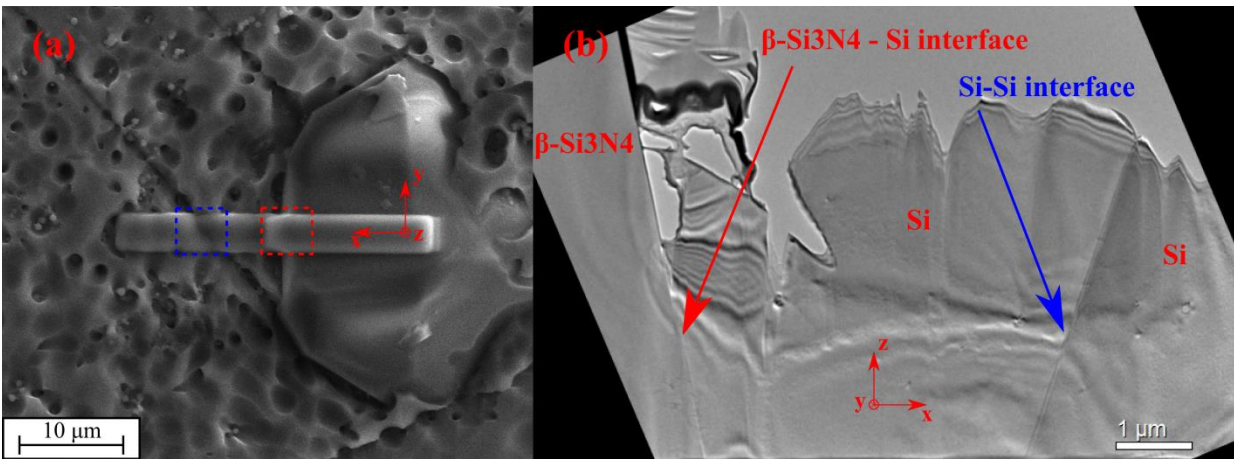


Figure 4 (a) Micrograph of sample area taken with the ion beam in the FIB. A carbon pad has been deposited on the sample area to protect the surface layer from ion beam damage during the rest of the sample preparation. The two areas of interest are also indicated, with the β -Si₃N₄ – Si boundary indicated in red and the Si-Si GB indicated in blue. (b) TEM BF micrograph of the sample area.

3.2. The Si / β -Si₃N₄ orientation relation

The orientation relationship between Si and β -Si₃N₄ was found using the procedure described in [14]. The method consist of finding diffraction patterns (DP) for the two phases at two different tilt settings and mapping these in a stereographic projections to identify low index zones axis which overlap.

In Figure 5 (a) the BF micrograph of the Si – β -Si₃N₄ interface for one tilt setting is shown, along with the corresponding DP's from each of the two phases. For this tilt the sample is in the “edge on” orientation, which means that the electron beam is parallel to the interface plane. The Si DP is the [143] zone axis, while the β -Si₃N₄ is $[\bar{1}2\bar{1}0]$. From the DP's in Figure 5 it is also seen that the (0001) plane of β -Si₃N₄ and the (1 $\bar{1}$ 1) plane of silicon are nearly parallel. The angular difference between the two planes was calculated to be 1.7°. The Si DP in Figure 5 (a) is not exactly on zone, but tilted 2.5° from the zone axis.

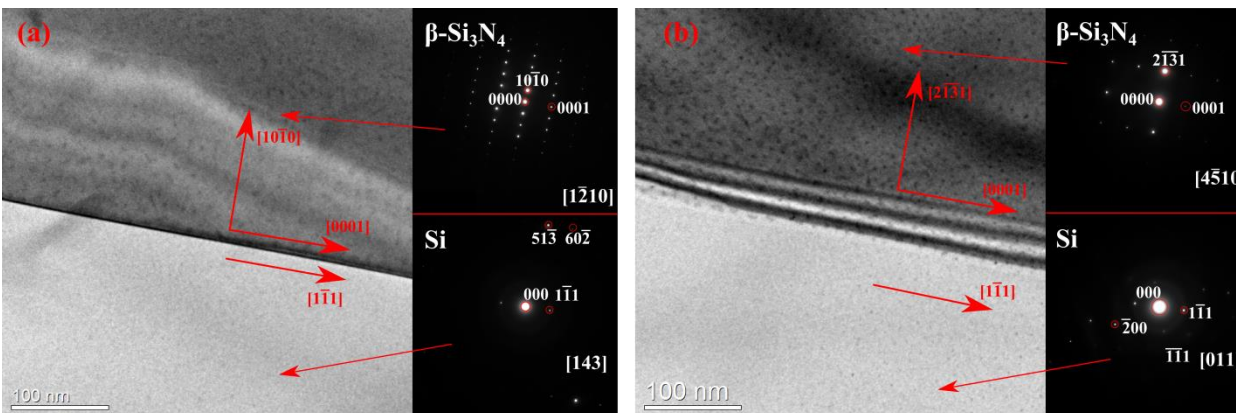


Figure 5 BF micrograph of the Si – β -Si₃N₄ interface with indexed DP's of the two phases for the (a) first tilt, DP's corresponding to [143]-Si and $[\bar{1}2\bar{1}0]$ - β -Si₃N₄, and (b) the second tilt, DP's corresponding to [011]-Si and $[\bar{4}5\bar{1}0]$ - β -Si₃N₄.

The BF micrograph and DP's of the two phases for the second tilt is shown in Figure 5 (b) tilted 19.4° from (a). Indexing the DP's gives the $[\bar{4}5\bar{1}0]$ zone axis for $\beta\text{-Si}_3\text{N}_4$ and $[011]$ for Si. As for the Si DP in Figure 5 (a), the DP from Si in Figure 5 (b) is also not exactly on zone. The tilt angle from the true zone axis is slightly bigger in this case, 5.1° . The Moirè fringes observed at the interface are due to that the two crystals overlap in the present projection since the interface plane is inclined to the electron beam.

The crystal directions found in Figure 5 (a) and (b) were plotted in two stereograms, one for $\beta\text{-Si}_3\text{N}_4$ and one for Si. These were aligned on top of each other so that the directions from the DPs in Figure 5 overlapped. In Figure 6 the combined stereogram of the $[\bar{4}5\bar{1}0]$ and $[143]$ pole is shown from $\beta\text{-Si}_3\text{N}_4$ and Si, respectively. It is seen that there is a low index zone axis from each phase that overlap, namely the $[0001]$ and $[1\bar{1}1]$ for $\beta\text{-Si}_3\text{N}_4$ and Si, respectively. From this stereogram it is seen that an OR between Si and $\beta\text{-Si}_3\text{N}_4$ exists. The OR can be described as

$$[0001] \beta - \text{Si}_3\text{N}_4 \parallel [1\bar{1}1] \text{Si}$$

$$(\bar{4}5\bar{1}0) \beta - \text{Si}_3\text{N}_4 \parallel (011) \text{Si}$$

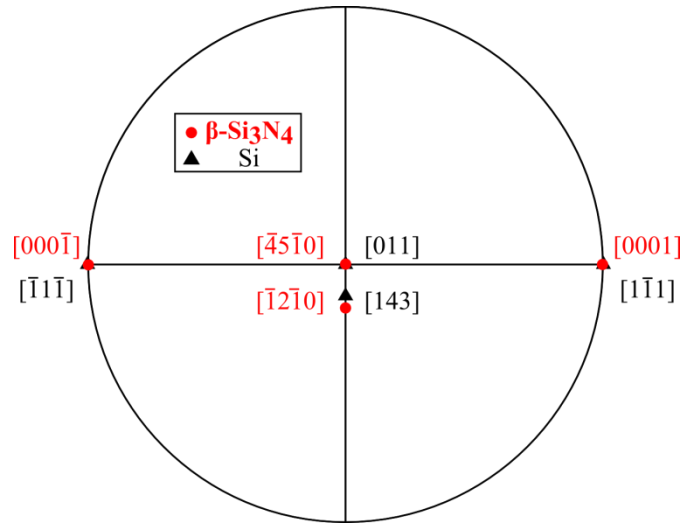


Figure 6 Stereogram constructed by overlapping the $[0001]$ stereogram of $\beta\text{-Si}_3\text{N}_4$ and the $[1\bar{1}1]$ stereogram for Si.

3.3. High resolution of the Si / $\beta\text{-Si}_3\text{N}_4$ interface

From the BF micrograph shown in Figure 5 (a) it appears that the interface is strained. This is seen from the change in contrast along the interface compared to the bulk, as a consequence of the strain shifting the planes away from Bragg. To investigate this further, high resolution micrographs of the interface were obtained, shown in Figure 7. At this resolution it is apparent that the interface is strained. The strain can be quantified by comparing the lattice spacing close to the interface and those far away which are unstrained. The planes parallel to the interface are the easiest to analyze, as these have the largest lattice spacing which makes it simpler to identify

individual planes. These are the $(10\bar{1}0)$ planes, which are perpendicular to the (0001) planes. The lattice spacing was found by averaging over several lattice planes. For the lattice spacing close to the interface the spacing was found by averaging over 5 planes, all of which are inside the strained region, while the lattice spacing further into the material were averaged over 10 planes. The strain in the interface will vary as a function of the distance from the interface, but the resolution in the image was not sufficient to plot this accurately. It was found that the lattice planes close to the interface were compressed by an average of 6.4% compared to with the lattice planes further away.

This strain is caused by the lattice mismatch between the interface planes of the two crystals. If the strain is compressive in one direction, then the strain in the perpendicular direction must be tensile, i.e. the unit cell of $\beta\text{-Si}_3\text{N}_4$ is stretched in the $[0001]$ direction. This fits with the fact that the lattice spacing of the $\{111\}$ Si planes is 3.14 \AA compared to 2.91 \AA for $(0001) \beta\text{-Si}_3\text{N}_4$. This is further indication that there is an epitaxial relation between the $\beta\text{-Si}_3\text{N}_4$ and Si, as no strain would be present if this was not the case.

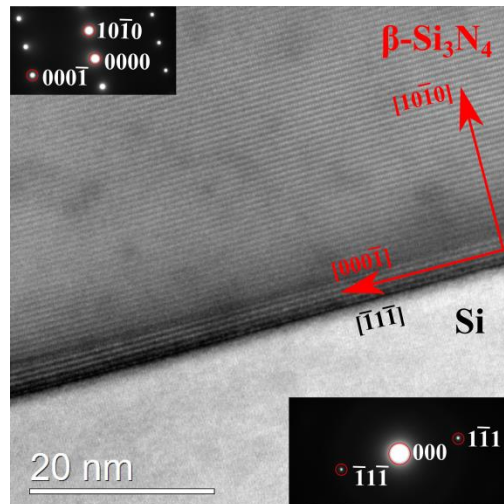


Figure 7 High resolution BF micrograph of the Si / $\beta\text{-Si}_3\text{N}_4$ interface

3.4. The Si / Si grain boundary

As seen in Figure 4 the sample also contained a Si GB. Due to the geometry of the sample it was not possible to tilt this GB to an “edge on” orientation. To determine what type of GB this is, a similar procedure as described in section 3.2 was used. Instead of overlapping the two grains and identifying the low index zone axis which overlap, the indexed orientation was mapped in the same stereogram. The GB is then identified by the rotation necessary to bring the planes and directions from one grain into coincidence with the other grain [14].

In Figure 8 a BF micrograph that contains the Si grain boundary is shown, along with the DPs from the two grains the same tilt. The grains were labeled as Grain 1 and 2, with Grain 1 corresponding to the Si grain on the left hand side in Figure 4 (b) and Grain 2 corresponding to

the one on the right hand side. At this tilt the grains were oriented along the $[011]$ and $[\bar{1}\bar{1}4]$ directions, for Grain 1 and Grain 2, respectively. For the second tilt, Grain 1 and 2 were oriented along the $[125]$ and $[1\bar{2}\bar{5}]$ zone axis respectively.

To determine the grain boundary type, the directions found from the DP's were mapped in a stereogram, shown in Figure 9. In this figure the directions belonging to Grain 1 are red, while those belonging to Grain 2 are blue. It is seen that the angle of rotation necessary to bring Grain 1 into coincidence with Grain 2 is 70.5° about the $[101]$ axis. This rotation corresponds to a twin boundary in a face centered cubic (fcc) crystal. In the notation of coincidence site lattice (CSL), this is known as a $\Sigma 3$ boundary. A 70.5° rotation around the $[101]$ axis is equivalent to a 60° twist around the $[111]$ direction, which is another often used designation for a $\Sigma 3$ boundary [15].

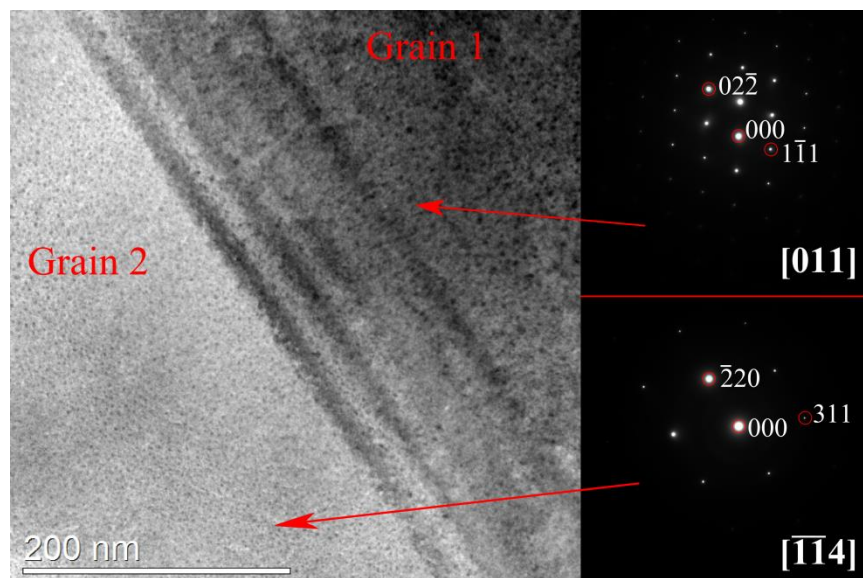


Figure 8 BF micrograph of the Si / Si grain boundary with the corresponding DP's

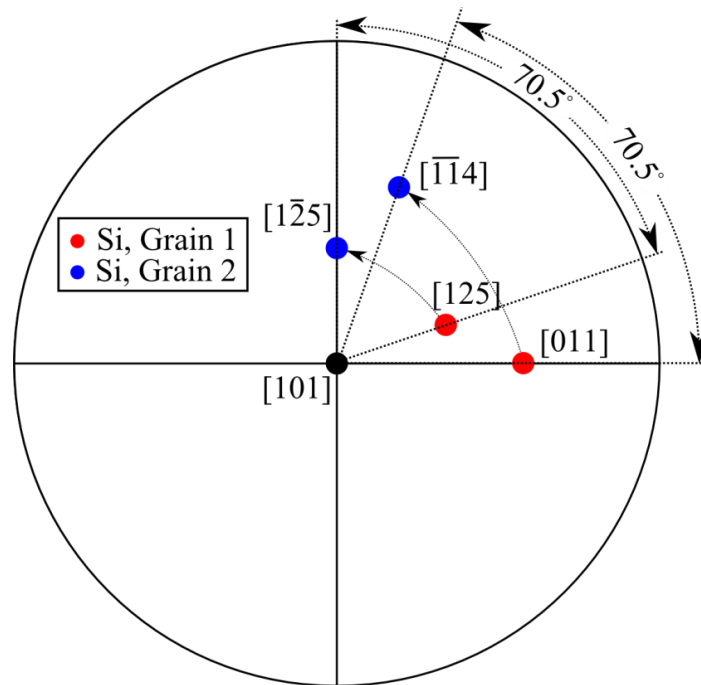


Figure 9 Stereogram of the crystal directions from the two Si grains for two different tilts. Also noted is the rotation about [101] necessary to bring one crystal into coincidence with the other.

3.5. Nucleation as a source of twins

From Figure 3 (a) it is seen that the two Si GBs are parallel, which means that the second GB is also a $\Sigma 3$ boundary. As stated previously, it is likely that Si nucleated on two of the facets of the particle. For a particle with the hexagonal symmetry, as we have for the β -particles, the angle between the normal of neighboring facets will be 60° . A $\Sigma 3$ boundary can be described as a 60° twist around the [111] axis. With the OR found in section 3.2, especially $[0001] \beta - Si_3N_4 \parallel [1\bar{1}1] Si$, the $\Sigma 3$ boundary is a result of the geometry of the particle, as the [0001] direction is perpendicular to the $(10\bar{1}0)$, (1100) , and $(01\bar{1}0)$ planes, which are the facets planes of a particle with this hexagonal symmetry.

From the particles in Figure 3, it is seen that in all three cases the boundaries are parallel. This was observed from other particles as well. Parallel boundaries are often observed in mc-Si and are referred to as parallel twins, as the GBs are usually $\Sigma 3$ boundaries. Kutsukake et al. observed that these parallel twin boundaries could be traced back to the crucible wall, which in this case was where the growth started [16]. In previous work by our group it has been observed that these parallel twin boundaries often extend from clusters of β - Si_3N_4 particles [2]. This work suggests that a possible source of these parallel twins is the nucleation on β - Si_3N_4 particles.

From two of the particles in Figure 3, namely (a) and (c), it is seen that the angle of the GB and facet normal is different for the two particles. Assuming that this is a $\Sigma 3$ GB in the case of Figure 3 (c) as well, based on the argument above, then this implies two things; either that the grain boundary plane is different or that the parallel planes are different, i.e. that the relation $(4\bar{5}10) \beta -$

$Si_3N_4 \parallel (011) Si$ is not the same in every case. Future work should investigate if the OR relation described in section 3.2 holds for all particles where nucleation has occurred, and how it deviates if it does.

Examples of particles with three GBs were also found, although they were not that frequently observed. An example of this is shown in Figure 10. From the symmetry arguments above, it is expected that these GBs are $\Sigma 3$ boundaries as well, though this was not shown.

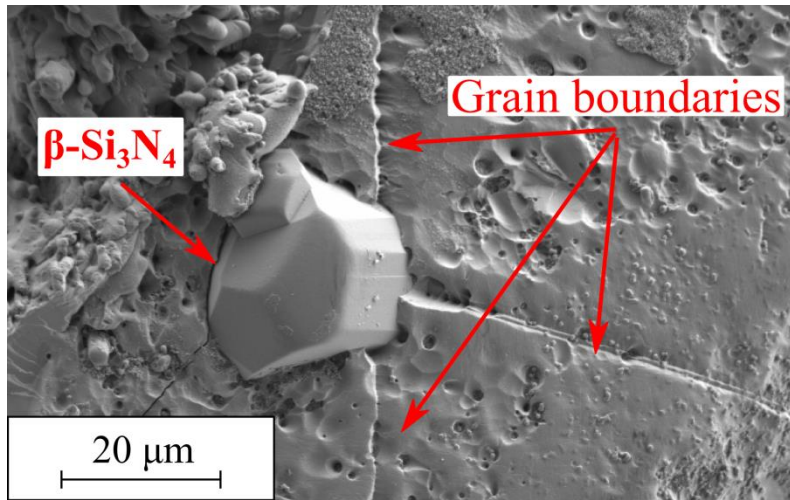


Figure 10 Example of $\beta-Si_3N_4$ particle with three GBs extending from it.

4. Conclusion

The orientation relation between Si and a $\beta-Si_3N_4$ particle found in a mc-Si ingot was investigated by TEM. A method for finding potential nucleation sites for TEM sample preparation of bottom cuts of mc-Si ingots was presented. A number of particles were identified, where it was argued that Si had nucleated on two different facets of the $\beta-Si_3N_4$ particles. The orientation relation was determined to be

$$[0001] \beta - Si_3N_4 \parallel [1\bar{1}1] Si$$

$$(\bar{4}5\bar{1}0) \beta - Si_3N_4 \parallel (011) Si$$

by analysis of diffraction patterns from the two phases. Further evidence for an epitaxial relation between Si and $\beta-Si_3N_4$ was found when examining the interface by high resolution. It was found that the interface was strained, and that this matched the expected strain and mismatch when considering an epitaxial relationship between the (0001) planes in $\beta-Si_3N_4$ and the {111} planes in Si.

A Si/Si grain boundary was also investigated. The origin of this GB was due to the nucleation occurring on two facets of the $\beta-Si_3N_4$ particle. This GB was determined to be a $\Sigma 3$ boundary. Nucleation of Si on $\beta-Si_3N_4$ was discussed as a source of twins in mc-Si.

References

- [1] E. Undheim, K.E. Ekstrøm, L. Arnberg, R. Holmestad, M. Di Sabatino, The effect of holding time on the size distribution of β -Si₃N₄ particles and nucleation undercooling in multicrystalline silicon, *Physica status solidi (c)* 13(10-12) (2016) 822-826.
- [2] K.E. Ekstrøm, E. Undheim, G. Stokkan, L. Arnberg, M. Di Sabatino, Beta-Si₃N₄ particles as nucleation sites in multicrystalline silicon, *Acta Materialia* 109 (2016) 8.
- [3] P. Goodman, M. O'Keeffe, The space group of beta-Si₃N₄, *Acta Cryst.* B36 (1980) 2891-2893.
- [4] A. Kuwabara, K. Matsunaga, I. Tanaka, Lattice dynamics and thermodynamical properties of silicon nitride polymorphs, *Phys. Rev. B* 78 (2008) 064104.
- [5] D.P. Thompson, The crystal chemistry of nitrogen ceramics, *Materials Science Forum* 47 (1989) 21-42.
- [6] M. Yashima, Y. Ando, Y. Tabira, Crystal structure and electron density of alpha-silicon nitride: Experimental and theoretical evidence for the covalent bonding and charge transfer, *Journal of Physical Chemistry* 111 (2007) 3609-3613.
- [7] Y. Inomata, T. Yamane, beta-Si₃N₄ Single crystals grown from Si melts, *Journal of crystal growth* 21 (1974) 317-318.
- [8] H.M. Jennings, Review on reactions between silicon and nitrogen, *Journal of Materials Science* 18 (1983) 951-967.
- [9] M. Yang, R.Q. Wu, W.S. Deng, L. Shen, Z.D. Sha, Y.Q. Cai, Y.P. Feng, S.J. Wang, Electronic structures of beta-Si₃N₄ (0001)/Si (111) interfaces: perfect bonding and dangling bond effects, *Journal of Applied Physics* 105 (2009).
- [10] E. Bauer, Y. Wei, T. Müller, A. Pavlovska, I.S.T. Tsong, Reactive crystal growth in two dimensions: Silicon nitride on Si(111), *Physical review B* 51(24) (1995).
- [11] H. Ahn, C.L. Wu, S. Gwo, C.M. Wei, Y.C. Chou, Structure determination of the Si₃N₄/Si(111) - (8x8) surface: A combined study of kikuchi electron holography, scanning tunneling microscopy, and ab initio calculations, *Physical review letters* 86(13) (2001).
- [12] T.E. Quested, A.L. Greer, Athermal heterogeneous nucleation of solidification, *Acta Materialia* 53 (2005) 2683-2692.
- [13] K. Kelton, A.L. Greer, *Nucleation in Condensed Matter: Applications in Materials and Biology*, Pergamon 2010.
- [14] D.B. Williams, C.B. Carter, *Transmission Electron Microscopy*, Chapter 18, Springer 2009.
- [15] S. Ratanaphan, Y. Yoon, G.S. Rohrer, The five parameter grain boundary character distribution of polycrystalline silicon, *J. Mater. Sci* 49 (2014) 4938-4945.
- [16] K. Kutsukake, Abe T., Usami N., Fujiwara K., K. Morishita, K. Nakajima, Formation mechanism of twin boundaries during crystal growth of silicon, *Scripta Materialia* 65 (2011) 556-559.